Release behavior of hydrogen isotopes in Li_2TiO_3 pellet

Deqiong Zhu, Takuji Oda and Satoru Tanaka

Department of Nuclear Engineering and Management, The University of Tokyo

(Received: 25 May 2012 / Accepted: 20 August 2012)

Release behavior of hydrogen isotopes thermally sorbed in Li_2TiO_3 pellet was studied by thermal desorption spectroscopy (TDS). As microstructure (grain size, surface condition, open and closed pores) of pellet samples were changed by high-temperature sintering, the release behavior of hydrogen isotopes was changed. The amount of hydroxyl groups chemically adsorbed on the surface was found to increase with the specific surface area. The gas migration in open pores was delayed to high temperature region (450~650 K), for which Knudsen diffusion and interaction between gas molecules and walls of narrow open pore channels is considered to be the main mechanism. The release of hydroxyl groups absorbed in the bulk was delayed due to the existence of closed pores, and these hydroxyl groups have to undergo bulk diffusion and trapping in closed pores several times before desorption.

Keywords: tritium breeder, hydrogen isotopes, Li_2TiO_3, pellet, microstructure

1. Introduction

The tritium release in ceramic breeder materials is a complex process, in which the contributions of bulk diffusion, surface processes and interaction with radiation defects were included as investigated in previous studies [1-4]. Just a few literatures were reported on the influence of porosity on tritium release behavior. Tanifuji et al. investigated the porosity dependence of tritium release in neutron-irradiated Li_2O sintered pellets. It was shown that the tritium release behavior is significantly affected even by a slight porosity change in pellet sample with densities above 87% T.D., and that tritium release can be delayed due to trapping in closed pores [5]. Peeters et al. compared the tritium residence time of different Li_2TiO_3 sample materials in the experiments EXOTIC-8 and EXOTIC-9/1, and suggested that tritium release improves with increasing open porosity and the closed porosity has no effect on tritium release behavior [6]. Tam et al. developed a random-lattice approach to study the tritium percolation through porous ceramic breeders by modeling the short range transport in pores via a convection-diffusion-reaction approach and long range transport via a matrix technique [7].

In the present work, Li_2TiO_3 pellet samples with different microstructure (grain size, specific surface area, open and closed pores) were prepared. The release behavior of hydrogen isotopes thermally sorbed in pellet samples was studied by thermal desorption spectroscopy (TDS). Scanning electron microscope (SEM, JSM-6510LA, JEOL, Ltd.) was used to observe the pore morphology and grain size. Mercury intrusion porosimetry (autopore(R) IV 9520, Micromeritics Instrument Corporation) was adopted to measure the open porosity, open pore size distribution. The specific surface area was measured by BET (Kr adsorption at 77 K) on an Autosorb-1-C (Quantachrome.Co). The influence of microstructure (grain size, specific surface area, open and closed pores) on hydrogen isotopes release behavior was discussed.

2. Experiment

Li_2TiO_3 pellet samples were prepared by pressing the powder into pellet and sintering. The starting materials of Li_2TiO_3 poly crystal powder, PVA (5 wt%) and stearic acid (5 wt%) were ball-milled for 6 h and mixed homogeneously. The mixture of powders was pressed into pellets stepwise at 20 kN (2 minutes), 40 kN (2 minutes) and 60 kN (2 minutes) per 1.3 cm^2. By sintering the as-prepared pellets in air at different temperatures for 12 h, five pellet samples of various apparent densities (% of theoretical density: 3.43 $g.cm^{-3}$ for Li_2TiO_3) were obtained: (a) 76% T.D., 1173 K, (b) 83.5% T.D., 1223 K, (c) 86.6% T.D., 1273 K, (d) 88.6% T.D., 1373 K and (e) 88.6% T.D., 1473 K. Note that these apparent densities were evaluated by measuring the mass and size of pellets. The color of all the pellet samples is white after sintering in air at high temperatures.

Deuterium was incorporated into pellet samples by heating in 100 Pa D_2O vapor at 1073 K for 1 h in absorption system. After cooling down and evacuation, the samples were transferred into a high-vacuum TDS system, and then were heated to 973 K at 5 K/min for TDS experiment. TDS spectra of released gas versus temperature or time were obtained during the heating process. Figure 1 shows the photographs of five pellet

zhudeqiong@flanker.n.t.u-tokyo.ac.jp

samples after TDS experiments. The gray color in samples (a) and (b) and darker color in samples (c) to (e) were observed. It was reported that Li containing species (Li and LiOD) were observed in mass spectra for Li_2TiO_3 by heating above 973 K in D_2O atmosphere. And the color of Li_2TiO_3 changed from white to light blue after heated in D_2O atmosphere, which was attributed to be due to the oxygen defects induced by LiOD vaporization [8]. In the present work, the color of Li_2TiO_3 pellet samples changed to gray or black after heated in 100 Pa D_2O vapor, which is similarly considered to be induced by reduction.

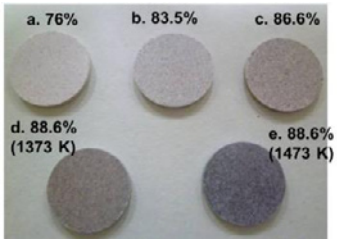

Fig. 1 Photographs of pellet samples after TDS experiment

3. Results and discussion

3.1. Release behavior of hydrogen isotopes

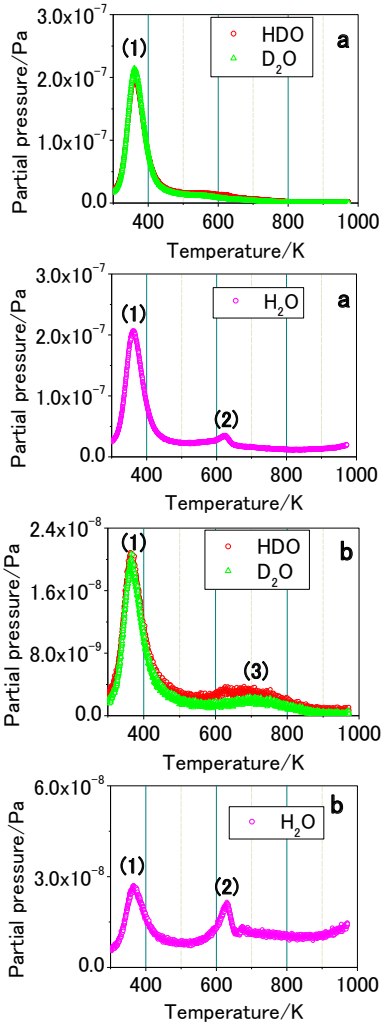

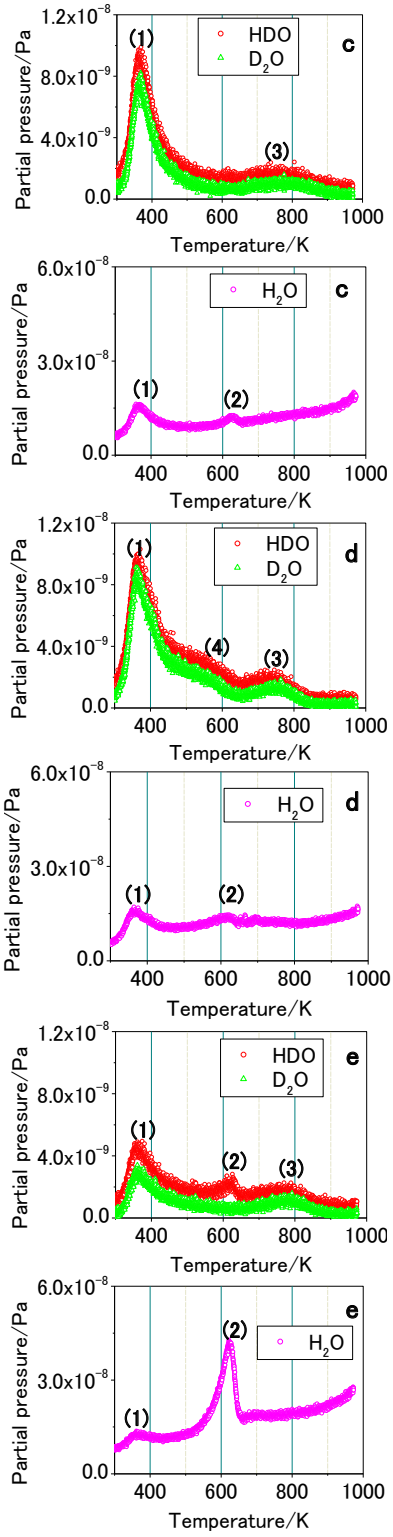

Fig. 2 TDS spectra for Li_2TiO_3 pellet samples: (a) 76% T.D., (b) 83.5% T.D., (c) 86.6% T.D., (d) 88.6% T.D. (1373 K), (e) 88.6% T.D. (1473 K)

Figures 2 show the TDS spectra for Li_2TiO_3 pellet samples. Deuterium thermally sorbed in pellet samples was released mainly in HDO and D_2O. One peak was observed at around 360 K for HDO, D_2O and H_2O, named peak (1). For H_2O, one more peak was observed at around 625 K, named peak (2). Except sample (e), no obvious HDO

release corresponding to peak (2) was observed. A peak for HDO and D_2O was observed at 650~900 K in samples (b) to (e), named peak (3). In sample (d), a broad peak between peak (1) and peak (3) was observed at 450~650 K for HDO and D_2O, named peak (4). For peak (3) and peak (4), no obvious H_2O peak was observed.

Based on the previous studies [9, 10], peak (1) is assigned to molecules physically adsorbed on the surface, which is released through desorption of physically adsorbed water molecules and migration along open pore channels, and peak (2) to hydroxyl groups chemically adsorbed on the surface, which is released by recombination desorption or isotope exchange reactions. In order to assign peak (3) and peak (4), the D/H ratios for peaks (1) to (4) were calculated and compared in Table 1. For peaks (3) and (4), no H_2O peak was obviously observed, which could be submerged in the high-level background. In order to give more precise evaluation of D/H ratios for peaks (3) and (4), the H_2O peak was estimated from HDO and D_2O peaks by assuming the equilibrium for the following reaction:

$$H_2O + D_2O = 2HDO \quad (1)$$

The D/H ratios for peaks (4) and (5) evaluated without (shown in brackets) and with considering the estimated H_2O peaks were compared.

Table 1 D/H ratios for peak (1) to peak (4)

Sample	D/H ratio			
	peak (1) ~ 360 K	peak (2) ~ 625 K	peak (3) 650~900 K	peak (4) 450~650 K
a	0.96	-	-	-
b	0.91	-	1.8 (2.8)	-
c	0.82	-	1.9 (2.9)	-
d	0.89	-	1.9 (2.9)	1.9 (2.9)
e	0.86	0.01	1.9 (2.9)	-

The D/H ratio reflects the probability of isotope exchange reaction between deuterium species (D_2O, HDO, -OD) and H_2O residue in TDS system. For peak (1), isotope exchange reaction between released molecules (HDO, D_2O) and H_2O/-OH residue in TDS system partially occurred. For peak (2) with the lowest D/H ratio of around 0.01, it is considered that isotope exchange reaction between –OD on the sample surface and H_2O residue in TDS system largely happened. The D/H ratios for peak (3) and peak (4) are larger than that for peak (1) and peak (2), and similar to that of D_2O tank (D/H ratio=1.8). It indicates that the probability of isotope exchange reaction is much smaller in peak (3) and peak (4), which suggests that the origins of peak (3) and peak (4) are located at some places where residual H_2O gas in TDS system hardly reaches. In the present experiment, obvious H_2O peak with higher level than HDO and D_2O was observed at around 625 K. Three possibilities were considered for this H_2O peak: (i) –OH formed due to H_2O residue in D_2O tank and then desorbed as H_2O after recombination, (ii) –OH formed by isotope exchange reaction between –OD on the sample surface and H_2O residue in TDS system and then desorbed as H_2O after recombination, and (iii) isotope exchange reaction between released molecules (HDO, D_2O) and H_2O residue in TDS system.

The quantitative analysis for peak (1), peak (2) and peak (3), and assignment of peak (3) and peak (4) will be discussed in detail in section 3.4.

3.2. SEM observation

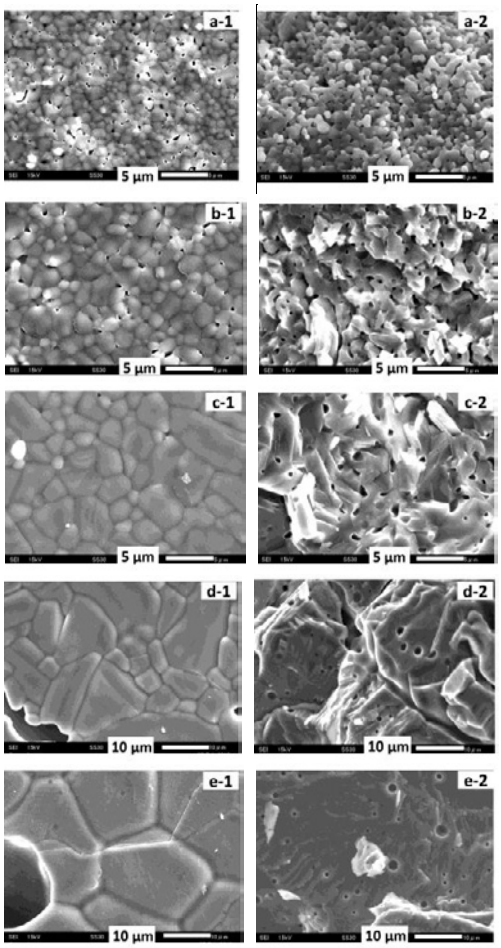

Fig. 3 SEM observation for Li_2TiO_3 pellet samples: (a) 76% T.D., (b) 83.5% T.D., (c) 86.6% T.D., (d) 88.6% T.D. (1373 K), (e) 88.6% T.D. (1473 K); 1- surface, 2- cross section

SEM observation for Li_2TiO_3 pellet samples is shown in Fig. 3. With the density increasing, grain sizes increased, and the porosity decreased. A broad grain size distribution was observed in sample (c) and especially obvious in sample (d) (Fig. 3.c-1 and d-1). Small pores with dead-end appeared in samples (b) to (e), and especially obvious in samples (d) and (e) (Fig. 3.b-2, c-2, d-2 and e-2). In samples (d) and (e), the grains in the bulk melted to form

big grain (Fig. 3.d-2 and e-2).

3.3. Mercury intrusion porosimetry

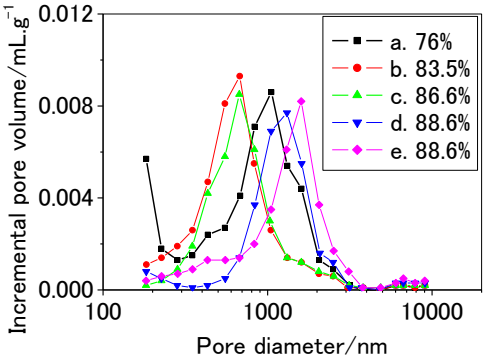

Fig. 4 Open pore size distribution for Li_2TiO_3 pellet samples: (a) 76% T.D., (b) 83.5% T.D., (c) 86.6% T.D., (d) 88.6% T.D. (1373 K), (e) 88.6% T.D. (1473 K)

The open porosity and open pore size distribution were measured by mercury intrusion porosimetry under the pressure of 6.8 MPa, for which pores smaller than 183 nm could not be measured. As a result, the open porosity and open pore size distribution could be underestimated to some extent. The open porosity was calculated from the open pore volume (volume of mercury intruded into sample) and external sample volume. The open porosity for pellet samples is: (a) 12.7%, (b) 11.9%, (c) 10.9%, (d) 9.8% and (e) 10.6%, which decreased from sample (a) to sample (d), and slightly increased in sample (e). Figure 4 shows the open pore size distribution, which was determined from the mercury pressure by the Washburn equation assuming that the geometry of pore channels can be approximated by cylindrical capillaries [11]. It seems that there are some pores smaller than 168 nm existing in pellet samples especially in sample (a). With the density increasing, the open pore size decreased in samples (b) and (c), and then increased in samples (d) and (e). With the sintering temperature increasing, the pores shrank first in samples (b) and (c), then expanded in samples (d) and (e) due to over-sintering at high temperature (1373 K and 1473 K). A small fraction of pores with larger size around several microns were also observed in sample (e). The closed porosity was evaluated from the measured open porosity and apparent density for pellet samples as *[closed porosity] = (1- [apparent density/theoretical density]) - [open porosity]*: (a) 11.3%, (b) 4.6%, (c) 2.5%, (d) 2.4% and (e) 0.8%. Due to the underestimation of open porosity by mercury intrusion porosimetry, the closed porosity might be overestimated especially in sample (a).

3.4. Discussion

3.4.1. Quantitative analysis for peak (1) and (2)

Table 2 shows the correlation between the specific surface area of pellet and the amount of peak (1) and peak (2). The amount of peak (1) (molecules physically adsorbed on the surface) was evaluated from the area of D_2O, HDO and H_2O peaks at around 360 K, and the amount of peak (2) (hydroxyl groups chemically adsorbed on the surface) was evaluated from the area of H_2O peak at around 625 K (HDO peak was added in sample (e)). The specific surface area of pellet samples was measured by BET.

Table 2 Correlation between specific surface area and amount of peak (1) and peak (2)

Sample	Specific surface area of pellet / $m^2 \cdot g^{-1}$	Peak (1) molecules/ 10^{17} g^{-1}	Peak (2) hydroxyl groups/ 10^{16} g^{-1}
a	0.762	22.5	11.2
b	0.120	2.2	6.4
c	0.035	0.9	1.3
d	0.058	1.1	1.5
e	0.039	0.4	19.8

The amount of molecules physically adsorbed on the surface (peak (1)) is proportional to the specific surface. Except sample (e), the amount of hydroxyl groups chemically adsorbed on the surface (peak (2)) is roughly proportional to the specific surface area in samples (a) to (d). It is considered to be due to that the concentration of surface defects induced by vaporization of Li-containing species is different in sample (e) sintered at the highest temperature (1473 K).

The vaporization characteristics of Li_2TiO_3 have been investigated by the mass spectrometric Knudsen effusion method, and it was shown that the vaporization of lithium-containing species increased with the temperature increasing [8, 12]. Hoshino et al. investigated the vaporization of lithium containing species under different atmospheres (D_2, D_2O, vacuum and O_2) from 973 to 1473 K [8], and the sum of partial pressures of Li-containing species (Li, LiO, Li_2O and LiOD) was found to be: $D_2 = D_2O >$ vacuum $> O_2$. In the present study, pellet samples were prepared by sintering in air, where Li_2TiO_3 should show an intermediate vaporization behavior between O_2 atmosphere and D_2O atmosphere due to the existence of moisture (H_2O, similar to D_2O) and O_2. In another work [13], the non-stoichiometry of Li_2TIiO_3 heated in reduction atmosphere was quantitatively analysed by thermogravimetry. The mass of Li_2TiO_3 was found to decrease with time and the weight loss due to Li_2O and O vaporization reached the maximum after heating at 1273 K for around 16 h in H_2 atmosphere. And the maximum weight loss due to Li_2O vaporization was found to be 0.982 mg of 288.5 mg, which results in Li_2O deficiency with molar fraction of 0.01. The amount of defects induced by sintering in air (without O vaporization) is considered to be smaller than this value in samples (a) to

(d), for which the influence from the defects on the release behaviour of hydrogen isotopes is considered to be negligible. However, the molar fraction of Li_2O might be close to or larger than 0.01 in sample (e) which was sintered at higher temperature (1473 K), and the influence of surface defects on the amount of surface hydroxyl groups is expected in sample (e).

Oda et al. [14] studied the influence of radiation defects on hydrogen isotope behavior in Li_2O by in situ IR absorption analysis, and suggested that hydrogen isotopes were stabilized in Li_2O through an interaction with the Li vacancy or mutual aggregation. Bikondoa et al. [15] used STM to image the reaction of water molecules with bridging-oxygen vacancies on rutile TiO_2 (110) and oxygen vacancies were visually observed being transformed into OH species as a water molecule dissociates in the vacancy. It indicates that oxygen vacancies act as active sites for hydroxyl groups. In the present work, defects induced by Li species vaporization might facilitate relatively larger amount of hydroxyl groups adsorbed on the surface, especially in sample (e).

3.4.2. Assignment of peak (3)

Peak (3) was observed at higher temperature region (650~900 K) than the peak due to hydroxyl groups chemically adsorbed on the surface in high-density pellet samples (d) to (e) and might located at some places where residual H_2O gas in TDS system hardly reaches. Here two kinds of possible origins for peak (3) are considered: (i) hydroxyl groups absorbed in the bulk, (ii) molecules trapped in closed pores. In order to clarify the origin of peak (3), the amount of molecules/hydroxyl groups for peak (3) was estimated from the area of D_2O and HDO peaks in TDS spectra, which is around 10^{15}.

In the case of (ii) molecules trapped in closed pores, the pressure needed to trap 10^{15} molecules was roughly estimated. By assuming the closed porosity in high-density pellet samples (d) to (e) to be 5%, the volume of closed pores is estimated to be around 0.005 cm^3 (the volume of pellet is around 0.1 cm^3). Based on the ideal gas law equation, around 800 Pa of D_2O vapor is needed to trap 10^{15} molecules at 300 K. However, 100 Pa D_2O vapor was applied in the present experiment. Here we can infer that molecules trapped in closed pores are not a main source of peak (3).

In the previous study, 7.8×10^{16} cm^{-3} hydroxyl groups were thermally absorbed in the bulk of Li_2TiO_3 single crystal plate after heating in 100 Pa D_2O vapor at 1073 K for 1 h [10]. The amount of hydroxyl groups for peak (3) is at the same level, which convinced us that peak (3) can be assigned mainly due to (i) hydroxyl groups absorbed in the bulk.

In order to make clear the release path for peak (3), the "effective grain size" is defined to be an effective diffusion length needed to reach the surface (or open pores). The "effective grain size" is calculated from temperature of peak (3) by using a simple diffusion model, the detail of which was reported in the previous study [9]. The real grain size of pellet samples was decided by SEM observation. Table 3 shows the correlation between the real grain size and "effective grain size". The "effective grain size" is several times larger than the real grain size. It indicates that hydroxyl groups might experience bulk diffusion in multiple grains due to the existence of closed pores. It is generally known that the migration along the grain boundaries is fast. The surface processes are considered to proceed fast at the temperature region of peak (3) (650~900 K) (the peak was observed at 625 K in the present work). Besides, peak (3) was not observed in 5 μm and 50 μm single crystal powder samples [10]. Accordingly, the release of hydrogen isotopes is considered to be jointly controlled by diffusion in the bulk, trapping in the closed pores and dissolution in the grains at the temperature region of peak (3). When the hydroxyl groups come to the surface of closed pores, molecules desorbed from the grain surface can be trapped in the closed pores, dissolve in grain and diffuse in the grain bulk again. After several-times bulk diffusion and trapping in closed pores, the hydroxyl groups can arrive at the surface of pellet or open pores and finally be released to the TDS system. No obvious dependence of hydrogen isotopes release temperature on the grain sizes decided by SEM was observed in the present work.

Table 3 Correlation between the real grain size and "effective grain size" for peak (3)

Sample	Real grain size/ μm	Peak temperature / K	"Effective grain size"/ μm	"Effective grain size"/ real grain size
a	~ 1	-	-	-
b	1~3	700	12	4~12
c	3~10	775	50	5~14
d	>5	750	32	<6
e	>10	780	55	1~5

3.4.3. Assignment of peak (4)

For peak (4) detected in sample (d), a similar peak also appeared between peak (1) and peak (2) in 5 μm (av.) Li_2TiO_3 single crystal powder sample, in which sever agglomeration was observed [10]. The possible origin of water molecules physically adsorbed on the surface of inner open pores is considered, which is released through migration along complicated-structure pore channels. In the simulation by using the random-lattice approach

developed by Tam, in which convection-diffusion-reaction approach was considered for short range transport in open pores, a sharp pulse of tritium-bearing species was injected at the center of interconnected pores. And the release of injected tritium-bearing species exhibited a broad distribution with the long tail, which indicates many different pathways through which the gas molecule can reach the outlet from the source [7]. In the present work, two kinds of open pore channels are assumed: (I) pore size much larger than molecule mean free path, (II) pore size smaller than molecule mean free path. In the case (I), interaction between gas molecules and walls of pore channels is negligible, and the gas diffusion is fast, which is released in peak (1). In the case (II), interaction between gas molecules and walls of pore channels has to be taken into account. The broad peak (4) is considered to be mainly due to Knudsen diffusion and interaction between gas molecules and walls of different-shape narrow open pore channels [16, 17]. It was reported that Knudsen diffusion is dominant in pores with size of several (tens) nm [18, 19]. In the present study, no obvious peak (4) was observed except sample (d). Hence, we may think that narrow pore channels were evolved in the sintering condition of sample (d). However, small pore channels of several (tens) nm could not be measured by mercury intrusion porosimetry. The detailed mechanism for peak (4) needs further study.

4. Summary and Future work

The release behavior of hydrogen isotopes thermally sorbed in Li_2TiO_3 pellet was studied by TDS. The release behavior of hydrogen isotope was obviously changed due to the change in the microstructure of materials by high-temperature sintering. The amount of hydroxyl groups chemically adsorbed on the surface increases with the specific surface area. The release of hydroxyl groups in the bulk was delayed due to the existence of closed pores through undergoing bulk diffusion in multi-grains and trapping in closed pores several times. The peak related to gas migration in open pores was observed at relatively high temperature region (450~650 K), which is considered to be due to Knudsen diffusion and interaction between gas molecules and walls of narrow open pore channels, which needs further study.

References

[1] Peter C. BERTONE, The kinetics that govern the release of tritium from neutron-irradiated lithium oxide, J. Nucl. Mater. 151 (1988) 281-292.

[2] A. RENÉ RAFFRAY, Seungyon CHO, Mohamed A. ABDOU, Modeling of tritium transport in ceramic breeder single crystal, J. Nucl. Mater. 210 (1994) 143-160.

[3] M. Oyaidzu, H. Kimura, A. Yoshikawa, et al., Correlation between annihilation of irradiation defects and tritium release in neutron-irradiated lithium zirconate, Fusion Eng. Des. 81 (2006) 583–588.

[4] Makoto Oyaidzu, Yusuke Nishikawa, Taichi Suda, et al., Detrapping behavior of tritium trapped via hot atom chemical process in neutron-irradiated ternary lithium oxides, J. Nucl. Mater. 375 (2008) 1-7.

[5] Takaaki Tanifuji, Daiju Yamaki, Tadashi Takahashi, Akira Iwamoto, Tritium release from neutron-irradiated Li_2O sintered pellets: porosity dependence, J. Nucl. Mater. 283-287 (2000) 1419-1423.

[6] M.M.W. Peeters, A.J. Magielsen, M.P. Stijkel, J.G. van der Laan, In-pile tritium release behaviour of lithium metatitanate produced by extrusion–spheroidisation–sintering process in EXOTIC-9/1 in the high flux reactor, Petten, Fusion Eng. Des. 82 (2007) 2318–2325.

[7] S.W. Tam, V. Ambrose, Tritium percolation through porous ceramic breeders – A random-lattice approach, Fusion Eng. Des.17 (1991) 43-48.

[8] T. Hoshino, et al., Vapor species evolved from Li_2TiO_3 heated at high temperature under various conditions, Fusion Eng. Des. 81 (2006) 555–559.

[9] Deqiong Zhu, Takuji Oda and Satoru Tanaka, Effect of grain size on hydrogen isotope behavior in $LiNbO_3$, Fusion Sci. Technol. 60 (2011) 1147-1150.

[10] Deqiong Zhu, Takuji Oda, Yohei Shono, Satoru Tanaka, Study of hydrogen isotopes inventory in Li_2TiO_3, J. Nucl. Mater. Submitted.

[11] J. Van Brake1, S. Modrý, M. Svatá, Mercury Porosimetry: State of the Art, Powder Technol. 29 (1981) 1-12.

[12] Hamazo Nakagawa, Mitsuru Asano, Kenji Kubo, Mass Spectrometric Investigation of the Vaporization of Li_2TiO_3, J. Nucl. Mater. 110 (1982) 158-163.

[13] T. Hoshino, M. Dokiya, T. Terai, et al., Non-stoichiometry and its effect on thermal properties of Li_2TiO_3, Fusion Eng. Des. 61-62 (2002) 353-360.

[14] Takuji Oda, Yasuhisa Oya, Satoru Tanaka, Dynamic observation of the behavior of 3 keV D_2^+ irradiated into Li_2O using IR absorption spectroscopy, J. Nucl. Mater. 346 (2005) 306-311.

[15] Oier Bikondoa, Chi L. Pang, Roslinda Ithnin, et al., Direct visualization of defect-mediated dissociation of water on TiO_2 (110), Nat. Mater. 5 (2006) 189-192.

[16] Jaime Benítez, Principles and Modern Applications of Mass Transfer Operations (A JOHN WILEY&SONS,INC., New Jersey, 2009), p.59.

[17] Douglas M. Ruthven, Principles of Adsorption and Adsorption processes (A Wiley & Sons, New York, 1984), p 136.

[18] Kourosh Malek, Marc-Olivier Coppens, Knudsen self- and Fickian diffusion in rough nanoporous media, J. Chem. Phys. 119 (2003) 2801-2811.

[19] Aaron W. Thornton, Tamsyn Hilder, Anita J. Hill, James M. Hill, Predicting gas diffusion regime within pores of different size, shape and composition, J. Membrane. Sci. 336 (2009) 101-108.